Hindawi Publishing Corporation
Advances in Materials Science and Engineering
Volume 2016, Article ID 3048716, 11 pages
http://dx.doi.org/10.1155/2016/3048716

Research Article

The Effects of High Alkaline Fly Ash on Strength Behaviour of a Cohesive Soil

A. Binal

Faculty of Engineering, Department of Geological Engineering, Hacettepe University, Beytepe Campus, 06800 Ankara, Turkey

Correspondence should be addressed to A. Binal; adil@hacettepe.edu.tr

Received 28 February 2016; Revised 3 June 2016; Accepted 7 June 2016

Academic Editor: Guocheng Lv

Contemporarily, there are 16 coal-burning thermal power plants currently operating in Turkey. This number is expected to rise to 46 in the future. Annually, about 15 million tons of fly ash are removed from the existing thermal power plants in Turkey, but a small proportion of it, 2%, is recyclable. Turkey's plants are fired by lignite, producing Class C fly ash containing a high percentage of lime. Sulfate and alkali levels are also higher in Class C fly ashes. Therefore, fly ash is, commonly, unsuitable as an additive in cement or concrete in Turkey. In this study, highly alkaline fly ash obtained from the Yeniköy thermal power plants is combined with soil samples in different proportions (5%, 10%, 15%, 20%, and 25%) and changes in the geomechanical properties of Ankara clay were investigated. The effect of curing time on the physicomechanical properties of the fly ash mixed soil samples was also analyzed. The soil classification of Ankara clay changed from CH to MH due to fly ash additives. Free swelling index values showed a decrease of 92.6%. Direct shear tests on the cohesion value of Ankara clay have shown increases by multiples of 15.85 and 3.01 in internal friction angle values. The California bearing ratio has seen a more drastic increase in value (68.7 times for 25% fly ash mix).

1. Introduction

Nowadays, fly ash from a power plant is getting to be a more complicated issue for countries due to environmental problems. The number of thermal power plants in Turkey corresponds to energy needs that are increasing day by day. Turkish lignite is typically low-grade coal that has a very low calorific value and high mineral matter content [1–3]. It has been reported in various studies that extreme, high ash yields can range from 23% to 64% [4, 5], which produce vast quantities of coal fly ash to be disposed. According to the latest numbers, the total amount of ash in ponds and landfills has already reached around 100 billion tons in Turkey [3]. Yeniköy power plant uses 4.8 million tons of low-quality lignite and generates 1.2 million tons of ash per year [3]. In contrast, a small quantity of fly ash is used as additives to raw cement or concrete, with far more being stored in the field and ash dam. Therefore, there have been limited studies on the stabilization of cohesive soils with fly ash addition in Turkey.

Bituminous coals have low concentrations of calcium compounds, and the ash produced (Class "F") exhibits no self-cementing characteristics. Subbituminous coals have higher levels of calcium carbonate ($CaCO_3$); thus, the ash (Class "C") produced during combustion is rich in calcium, resulting in self-cementing characteristics. Since Class "C" fly ash is self-cementing; activators such as lime or Portland cement are not required. Upon exposure to water, Class "C" fly ash hydrates forming cementitious products similar to those produced during the hydration of Portland cement. This property makes self-cementing fly ash a very practical and economic stabilization agent for use in a variety of construction applications [6]. Some studies on the performance of fly ash mixed soil have claimed that Class C fly ashes are accomplished of ameliorating physicomechanical properties of cohesive soils [7–11]. Fly ash is used to stabilize fine-grained soils so that a stable working platform can be provided for highway construction equipment [7, 12–14]. Additives with calcium oxide produce flocculation in the layers of clay by the substitution of monovalent ions by Ca^{2+} ions. This balances the electrostatic charges of the layers of clay and reduces the electrochemical forces of repulsion between them. The adhesion of the particles of clay into flocks then occurs, giving

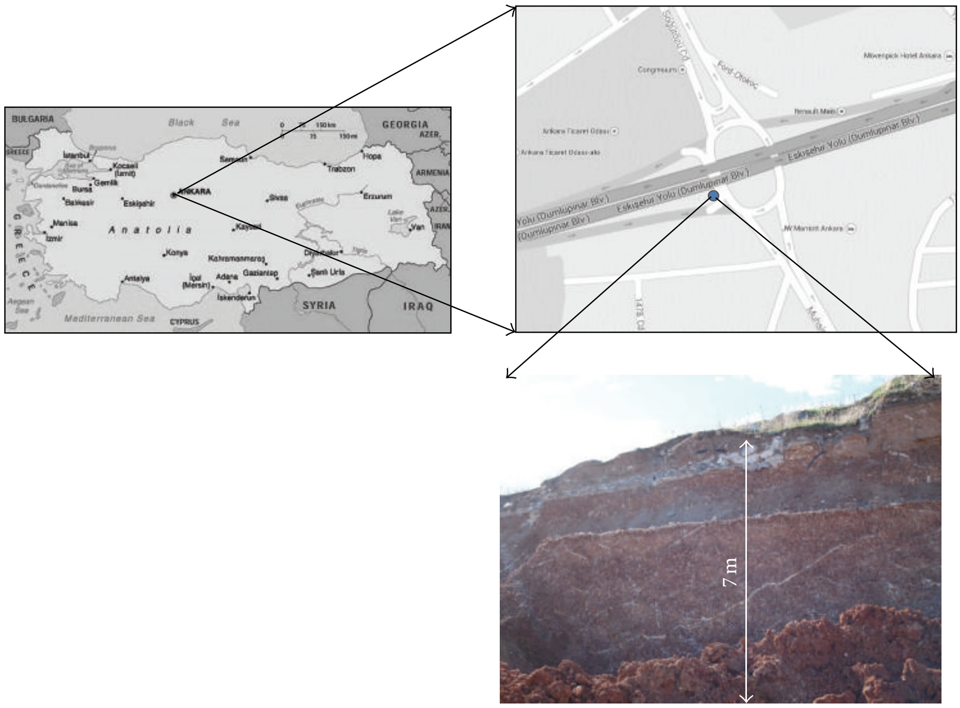

Figure 1: The soil sampling area.

rise to a soil with improved engineering properties: a more granular structure, less plasticity, greater permeability, and above all lower expansion [15–22]. Also, the presence of the OH^- ions produces an increase of the soil pH up to values of approximately twelve. In these conditions, pozzolanic reactions take place, when Si and Al which form part of the sheets of the clay dissolve and combine with the available Ca^{2+} giving rise to cementing compounds such as calcium silicate hydrates and calcium aluminate hydrates [18, 21, 23–25].

Akar et al. [3] have studied on short-term leaching manner of Fe, Ca, Cu, Co, Cd, Mn, Ni, Pb, Zn, and Cr (VI) from Yeniköy fly ash using TCLP-1311 [26] and ASTM D3987 [27] tests. According to their results, Ca was found as the most mobile element while Mn and Fe had the lowest mobility. The dissolution of selected trace elements was observed as higher for the particles below 38 μm size. For the leaching tests of original fly ash material, the highest solubility values were found for Ca, Pb, and Cr (VI), respectively. The results suggested that releases of these trace elements were all lower than the allowed limits for solid wastes imposed by the EC Directive [3]. Furthermore, as to the study by Turhan et al. [28], the utilization of the examined all fly ash samples (included Yeniköy fly ash) except Kangal and Soma, in the road, street, roadbeds, and road pavement does not pose any significant source of radiation hazard.

The other material of this study is Ankara clay that includes a sequence of lacustrine sediments that covers the surface of the Ankara Valley. These expansive soils are settled in western, central, and southern parts of Ankara, the capital of Turkey. Due to the expansive nature of this clay, damage to the roads and low-rise structures caused by differential volume changes of the clay occurs, particularly in the southern part of the city. This damage caused by the swelling has been deliberately ignored in both design and construction, however, because of limited budgets, poor construction methods, inadequate water drainage, and ineffective remedial measures [29].

Finer, reddish-brown clastic of the fluvial-lacustrine deposits is referred to as reconsolidate, stiff, and fissured "Ankara clay" in engineering, geological, and geotechnical studies. Networks of hair cracks and slickensides are often present in Ankara clay, and the surfaces of fragments are usually polished and glossy in nature. Undisturbed sampling is rather difficult, and specimens tend to fail along the fissures and irregular surfaces [30].

This work aims to investigate the possibility of using high alkaline fly ash from Yeniköy lignite-fired power station to ameliorate the geomechanical properties of Ankara clay. The effects of the proportions of the fly ash (FA) and curing time on the physical properties and strength development in Ankara clay have been illustrated in laboratory conditions. Scanning electron microscope (SEM) studies were performed to investigate the factors preventing swelling of Ankara clay. The outcomes of this work are to create new uses for FA in Turkey as well as build a basic mix design for further studies of strength and durability.

2. Materials

2.1. Ankara Clay. Three soil blocks have been supplied from a construction area, from a depth of three meters (Figure 1).

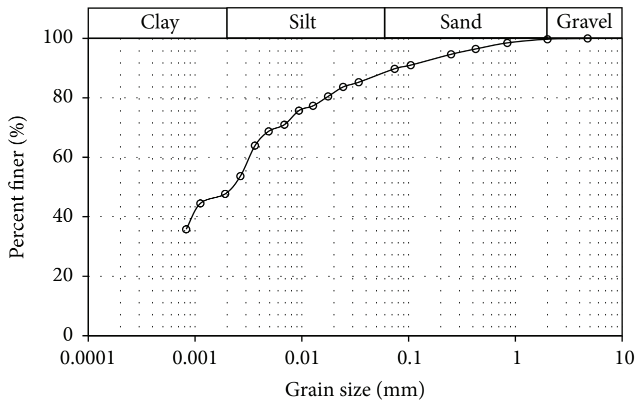

Figure 2: The particle-size distribution of AC.

The colour of Ankara clay (AC) in the sampling area is claret red or brown, and it includes lime bands.

AC includes 48% clay, 37.2% silt, 14.5% sand, and 0.3% gravel-sized materials (Figure 2). Regarding index properties, AC has a plastic limit (PL) of 35%, a liquid limit (LL) of 88.7%, and plasticity index (PI) of 53.7%. The soil sample was identified as "CH" by the unified soil classification system.

Smectite, illite, chlorite, kaolinite, quartz, and calcite minerals were determined by the XRD analysis of a bulk sample (range: 5°–70°) (Figure 3(a)). Besides, types of clay minerals were identified by the XRD analysis on the same sample (Figure 3(b)).

AC has a typical value that is close to active clay (A_c = 1.12 < 1.2) and a high swelling potential (free swell index = 50%); therefore, it has been described as expansive soil. Shear strength parameters were calculated as cohesion (c) of 13.9 kPa and internal friction angle (ϕ) of 10.70. Furthermore, the CBR value has been determined as 6.7%. All tests were realized to ASTM standards. Chemical analysis presented that the principal constituents of AC are silica, aluminium, calcium, and iron oxides. Lime bands in AC are the cause of the high calcium content (Table 1).

2.2. Yeniköy Power Plant Fly Ash. In this study, a very high lime fly ash was obtained from the second unit of Yeniköy coal-fired power plant. X-ray fluorescence (XRF) analysis was realized to classify the fly ash. Yeniköy fly ash (YFA) is over 10% reactive lime (21.80%) due to TS EN 197-1 [32] and Class W (calcareous fly ash). In contrast to the standard required in reactive silica, YFA does not comply with the 25% rule. According to ASTM C618 [34] of SiO_2+Al_2O_3+Fe_2O_3, 40.63% of CaO, less than 50% and more than 10% due to Class C (high lime) fly ash provide critical conditions. YFA, SiO_2+Al_2O_3+Fe_2O_3, well below 70% of the amount due, does not comply with the conditions required in TS 639 [33]. For TS EN 450 standards [31], the limit for SO_3 is 3%; the amount of SO_3 in the ash is above this limit (16.63%). Because the percentage of free lime is 1.48%, the 1.00% of the standard limit has been passed. Accordingly, the desired conditions of YFA do not entirely conform to the respective four standards (Table 2).

Table 1: The physicomechanical properties and the chemical composition of AC.

Index properties		Chemical composition (%)	
Natural water content, w_n (%)	30	SiO_2	56.35
Natural unit weight, γ_n (kN^3)	17.5	Al_2O_3	12.7
Liquid limit, w_L (%)	88.7	Fe_2O_3	5.37
Plasticity index, PI (%)	53.7	MnO	0.09
Specific gravity, G_s	2.69	MgO	1.99
Gravel (%)	0.3	CaO	9.2
Sand (%)	14.5	Na_2O	0.88
Silt (%)	37.2	K_2O	1.37
Clay (%)	48	TiO_2	0.81
Free swell index (%)	50	P_2O_5	0.12
% finer than number 200	89.8	LOI	11.12
Activity, A_c	1.12		
Mechanical properties			
Cohesion (kPa)	13.9		
Internal friction angle (°)	10.7		
California bearing ratio (CBR, %)	6.7		

The morphological analysis results show that usually semispherical and spherical glass beads have a grain size between 2.1 and 16.89 μm (Figure 4) as well as rough surfaces, both perfectly ball-shaped and irregularly shaped particulate (Figure 5). Its irregularly shaped particles are 10–60 microns big.

The natural pH value of fly ash is a valuable property which has a significant effect on the mobility of trace elements in an aqueous environment. Fly ash-water slurry was prepared by mixing 5 g of fly ash with 100 mL of deionized water for the determination of the pH value of the sample [3]. WTW brand (3110) pH meter was used to determine the pH of YFA at one-hour intervals for 24 hours' period. The 24 hours of pH was determined as 12.67. Specific gravity and surface area of YFA were determined as 2.63 and 0.169 m^2/g (Table 3).

XRD diffractograms show that YFA includes quartz, unburned clay remains (free lime), anhydrite, gehlenite, hematite, calcite, and sulphide (Figure 6).

3. Methods and Results

This study determined the effects of the fly ash (FA) additives on the strength of clay soil. AC was mixed with fly ash in 5%, 10%, 15%, 20%, and 25% proportions. Atterberg consistency limits, direct shear, the California bearing ratio (CBR), and swelling index tests were used on the cured samples, all tests to ASTM, and Indian standards. At the end of experiments, SEM imaging was realized on the samples.

3.1. Sample Preparation. The samples were prepared by the rules of modified proctor test sample preparation as to ASTM D1557 [35]. In that standard, soil at a selected moulding

Table 2: Standards compliance limits.

Oxide mass (%)		TS EN 450 [31]	TS EN 197-1 [32]		TS 639 [33]	ASTM C618 [34]	
			V	W		F	C
SiO_2	21.85						
Al_2O_3	15.41						
Fe_2O_3	3.36						
S+A+F	40.63				>70.00	>70.00	>50.00
CaO	28.54						
MgO	2.73				<5.00		
SO_3	16.63	<3.00			<5.00	<5.00	<5.00
K_2O	1.02						
Na_2O	6.87						
LOI	3.57	<5.00	<5.00	<5.00	<10.00	<6.00	<6.00
Cl^-	0.008	<0.10					

TS EN: Turkish and European standards; TS: Turkish standard.

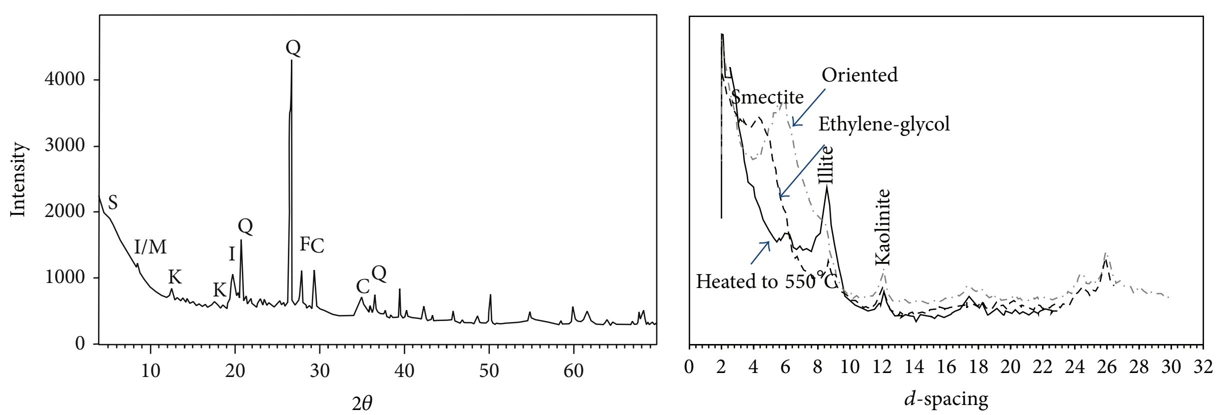

Figure 3: Typical XRD patterns of AC: (a) bulk (whole) sample and (b) clay fraction.

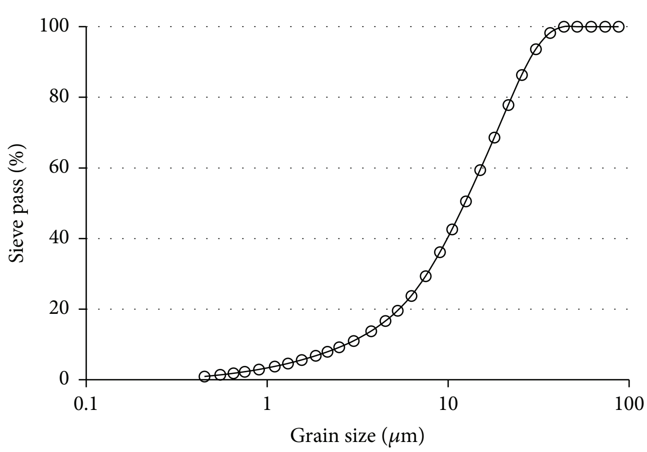

Figure 4: The grain size of it was determined by using Sympa Technology Laser Grain Size Analyses System.

water content is put in five layers into a mould, with each layer compacted by 56 blows of a 4.5 kg hammer dropped from a distance of 45 cm. The resulting dry unit weight is determined. The procedure is repeated for an adequate number of moulding water contents to establish a relationship between the dry unit weight and the moulding water content for the soil. The compaction curve is plotted with the values of the dry unit weight and water content. The values of the highest dry unit weight and optimum moisture content are found from the compaction curve [35]. All CBR tests of samples were realized in optimum moisture content value and about at 98% modified proctor stiffness. Therefore, modified proctor tests were carried out to determine optimum moisture content and maximum dry density of the mixed samples. During sample preparation, firstly, AC samples were ground and after that screened with #4 of a sieve which has 4.75 mm of the aperture. Undersize materials were mixed with 5%, 10%, 15%, 20%, and 25% of FA by weight at the optimum water content (Table 4). Then those mixes were poured into the CBR moulds which have

Table 3: Some physical properties of YFA.

Specific gravity (G_s)	Specific surface area (m^2/g)	pH
2.63	0.169	12.67

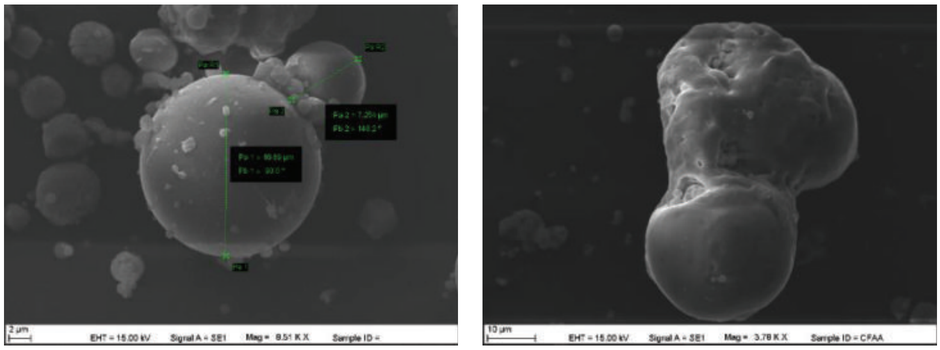

Figure 5: The scanning electron microscope (SEM) views of regular and irregular shaped glass beads of YFA.

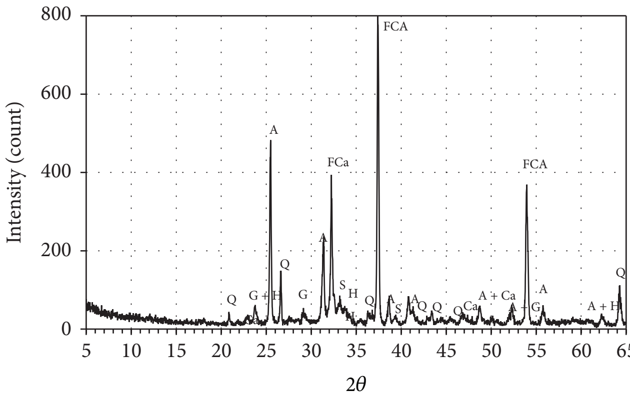

Figure 6: The X-ray diffractogram of YFA.

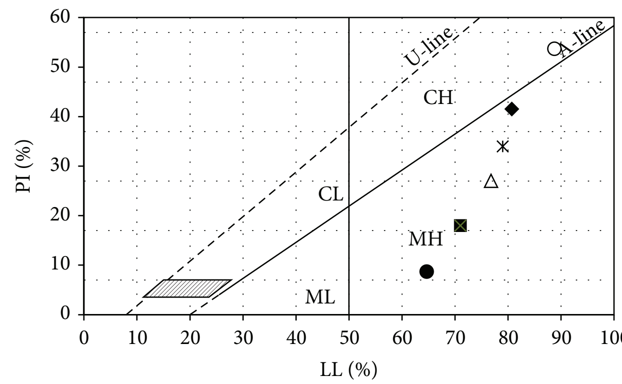

Figure 7: Consistency limits of AC and FA mixed soil.

152.4 mm in diameter and 177.8 mm of height. The samples were compacted in the five layers with 25 blows in each layer with using a mechanical compactor which automatically compacts and rotates mould after each blow while keeping track of the number of hammer blows. After that, mixtures were cured at 1, 7, and 28 days in the humidity cabinet which has 21°C of temperature and 90% of RH. During cure periods, prepared CBR samples have waited under load (7 kg), which present overburden pressure of the sampling depth of AC to prevent swelling and stress relaxation. Also, reference CBR samples having no FA were prepared as to the similar method of mixed samples.

3.2. Atterberg Limits. Atterberg limit tests were realized to examine the effects of the FA additive on the soil consistency. The 5%, 10%, 15%, 20%, and 25% fly ashes were mixed with AC. PI and LL tests were carried out to ASTM D4318 [36]. Results show that the FA additive is very active on the consistency limits of the soil. The unified soil classification of the AC was changed from "CH" to "MH." PI was decreased from 53.75% to 8.76%, and LL was reduced from 88.71% to 64.61% (Figure 7). Furthermore, the plastic limit increased

Table 4: Compaction characteristics of testing soil mixed with FA.

FA content (%)	The maximum dry unit weight, γ_d (kN/m^3)	Optimum water content (%)
0	17.85	30
5	16.85	31.5
10	15.84	32.1
15	15.15	32.53
20	14.72	33.33
25	14.17	34.84

from 34.96% to 55.85% with the FA additive. This result shows that the land becomes more pliable with FA's addition, better equipped for use in the construction of foundations and roads.

3.3. California Bearing Ratio (CBR). Prepared samples were tested as to the standard of the test method for California bearing ratio of laboratory compacted soils [37]. A fully automatic single-speed load frame that has 50 kN of the load cell and 1.27 mm/min speed was used in CBR tests. The values of California bearing ratio (CBR) tests show that the curing

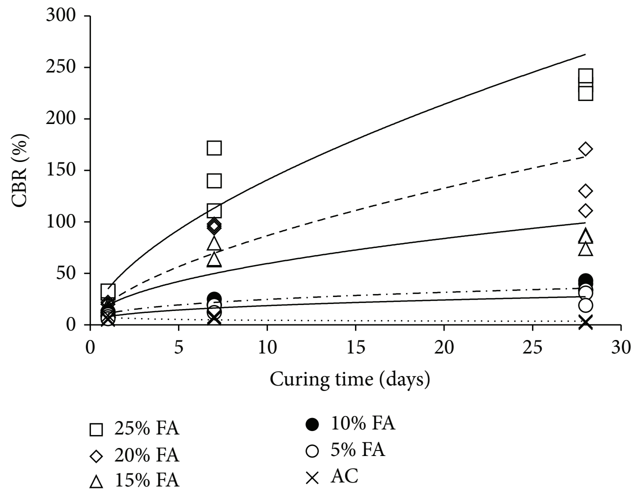

Figure 8: The effects of the curing time and FA content on the CBR values.

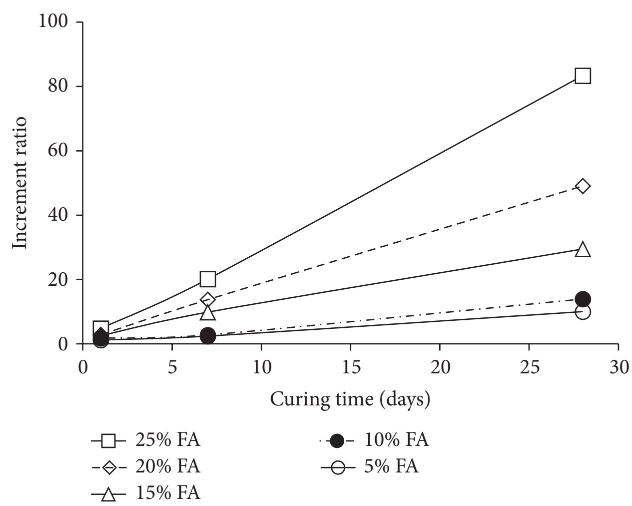

Figure 9: Increase at the CBR values with curing time and FA content.

time is critical to CBR values. All samples, including FA, present a high increase in CBR values after seven days curing (Figure 8). However, declines were observed in the CBR results of the samples, not including FA. That behaviour may be related to the curing conditions. Although AC samples were weighted with the load during curing, they started to swell when taking in water in the humidity cabinet. Therefore, they have begun to lose stiffness and CBR after the one-day curing. In contrast, other samples containing FA grew stiffer with curing time. The most increased rates (68.7 of 25% FA at 28 days) of the CBR values were found in the samples that include 25% FA (Figure 9). The increment ratio was calculated by dividing the CBR value of the FA mix by the CBR value of AC.

Furthermore, some physical changes were observed in the 25% FA mixtures. Although the colour of AC is claret red, the 25% FA mix colour was changed to a brownish green. As well, the 25% FA mix samples have shown brittleness (Figure 10).

Figure 10: The view of 25% FA mixes sample after the CBR test.

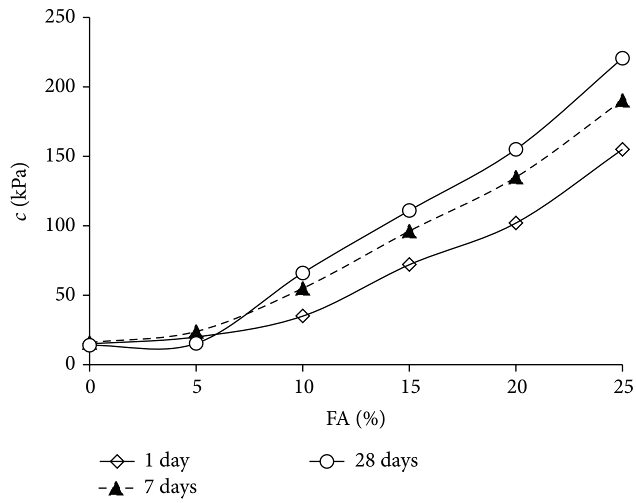

Figure 11: Variation of c with FA content and curing time.

3.4. Shear Strength. Shear strength properties of soil and fly ash mixed soil were determined by using direct shear test apparatus. Normal loads were decided as to sampling depth and overburden pressure. Furthermore, all tests were realized on 7- and 28-day cured samples according to standard test methods for a direct shear test of soils under consolidated drained conditions [38]. Due to the longer curing time, an increase in cohesion and angle of internal friction was determined to occur (Figures 11 and 12).

For 28-day curing period, AC's cohesion values increased 15.85 times and internal friction angles increased 3.01 times for the 25% fly ash mixed soil samples (Figure 13). Increment ratio was calculated by the value of the FA mix divided by the value of AC. Also the increase in internal friction angle is very striking. Fly ash additives roughen up to the surface of clay minerals and increase internal friction in that way.

3.5. Free Swell Index. Free swell is the increase in the volume of soil, without any external constraints, on submergence in water. The possibility of damage to structures because of swelling of expansive clays needs to be identified at the outset,

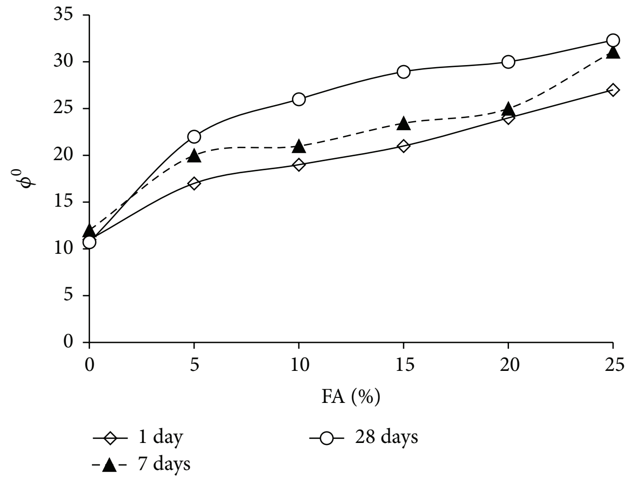

Figure 12: Variation of ϕ^0 with FA content and curing time.

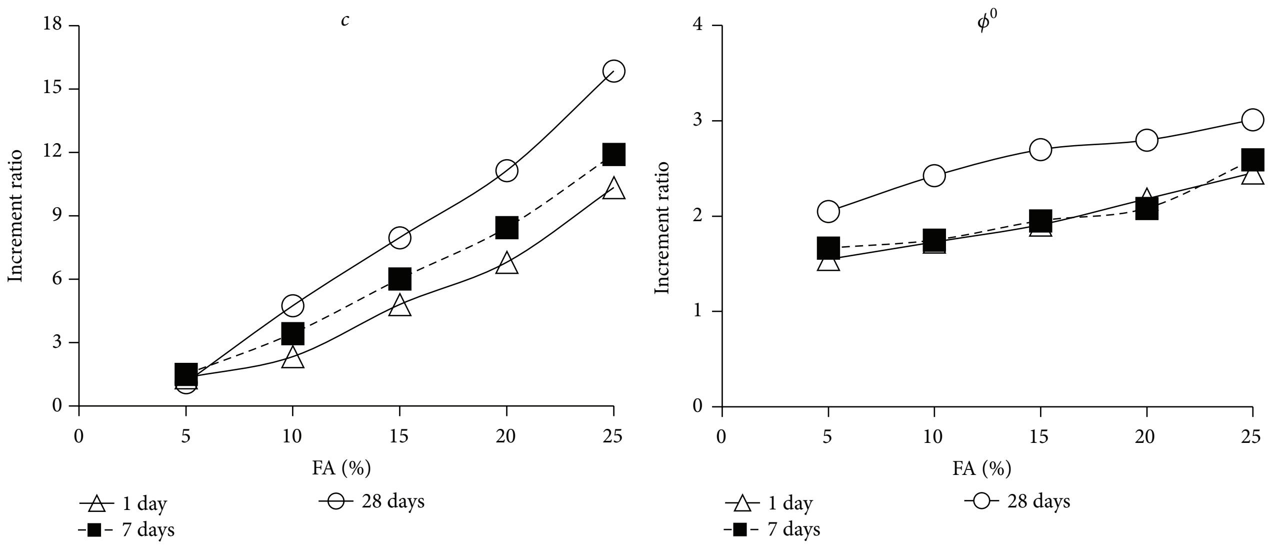

Figure 13: The increment ratios of shear strength parameters (c-ϕ) with FA and curing time.

for an investigation of those soils likely to possess undesirable expansion characteristics. Inferential testing is used to reflect the potential of the system to swell under different simulated conditions. The actual magnitude of swelling pressures developed depends on the dry density, initial water content, surcharge loading, and several other environmental factors. Swelling tests were carried out to the Indian standard [39]. In this procedure, two 10 g soil specimens of oven dry soil passing through a 425-micron IS sieve are taken. If highly swelling soils, such as sodium bentonite, the sample size may be 5 g, alternatively, a cylinder of 250 mL may be used. Each soil specimen shall be poured in each of two glass graduated cylinders (100 mL capacity). One cylinder shall be filled with kerosene oil and the other with distilled water up to a 100 mL mark. Then with removal of entrapped air by gentle shaking, the soils in both the cylinders shall be allowed to settle. Sufficient time which is not less than 24 h shall be allowed for the sample to attain an equilibrium state of the volume without any change in the volume of the soils. The final volume in each of the cylinders shall be read out. The level of the soil in the kerosene graduated cylinder shall be read as the original volume of the soil samples. The soil level in the distilled water cylinder shall be read as the free swell level [39].

The free swell index of the soil is calculated as follows:

$$\text{Free Swell Index (\%)} = \frac{V_d - V_k}{V_k} \times 100, \quad (1)$$

where V_d is the volume of soil specimen read from the graduated cylinder containing distilled water and V_k is the volume of soil specimen read from the graduated cylinder containing kerosene.

The free swell index values of soil samples decreased with the amount of fly ash in the mix (Figure 14). The free swell value of 25% fly ash mixed soil sample was close to 0%. With 5% FA mixed soil samples, the swelling ratio decreased by

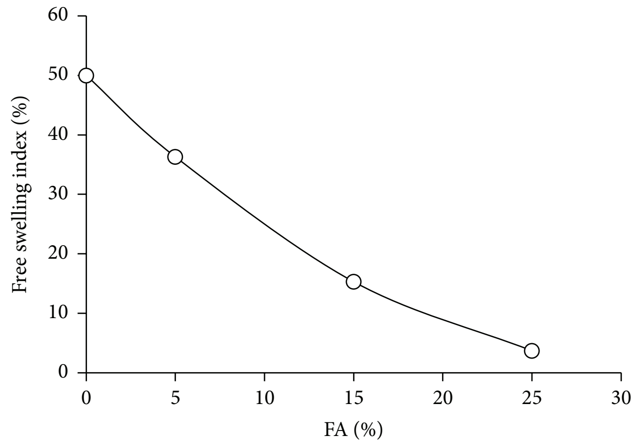

Figure 14: Free swelling index versus the amount of FA content.

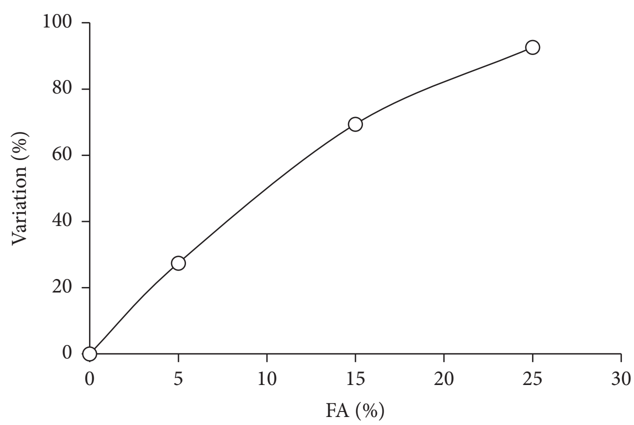

Figure 15: Free swelling variation versus the amount of FA content.

27.4% in value; with 25% FA, it declined by 92.6% (Figure 15). Clay soils, even with a very low rate of FA, can considerably reduce their swelling potential.

3.6. Scanning Electron Microscopy Study. After CBR tests, scanning electron microscopy (SEM) images of the samples were taken. In the SEM images, the clay surface was perfectly coated with fly ash among the grains. That explains why the swelling of the clay was prevented. Ash pellets move between the clay minerals with the water molecules and prevent swelling of the clay (Figure 16). Furthermore, FA grains are capable of making bonds among the clay minerals (Figure 17).

4. Statistical Evaluation

Multiple regression analyses were realized to obtain the relationships between shear strength parameters (c and ϕ) and fly ash content (FA, %) and curing time (d, days) as well as CBR values and fly ash content. XLSTAT of Addinsoft

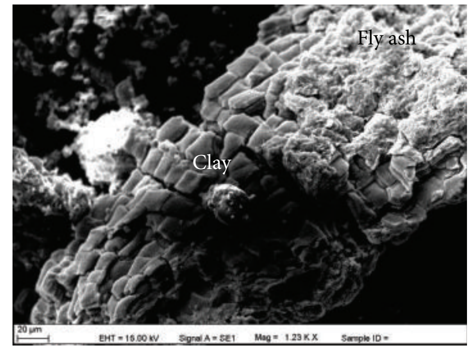

Figure 16: The SEM view of coated clay with ash pellets.

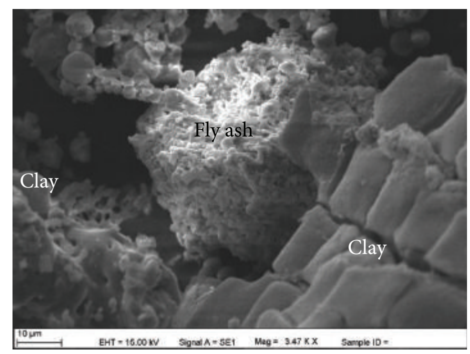

Figure 17: The view of ash particles that build the bridge between clay minerals.

was used to create the regression models. The best fit for estimating cohesion (c, kPa) was found as

$$c\,(\text{kPa}) = -19.445 + 1.068 * d + 708.642 * \text{FA},$$
$$\phi^{0} = 10.217 + 0.232 * d + 69.095 * \text{FA}, \quad (2)$$

where d is curing time (days) and FA is fly ash (%).

As well, the best model for CBR values was presented in

$$\text{CBR}\ (\%) = -37.173 + 2.32 * d + 5.039 * \text{FA}, \quad (3)$$

where d is curing time (days) and FA is fly ash (%).

The F-test was carried out to test the overall performance of the regression model (Table 5). Since $F_{\text{model}}(79.776, 50.485) > F_{(0.05,2,15)}(3.68)$ for shear strength parameters as well as $F_{\text{model}}(52.921) > F_{(0.05,2,51)}(2.79)$ for CBR or the P value is considerably smaller than $\alpha = 0.05$, the null hypotheses are rejected and as a result of that c, ϕ, and CBR related to d and FA.

The proportion between the regression sum of the square (SS_R) and the corrected total sum of squares is called the coefficient of determination (R) and is often used to judge the adequacy of a regression model [40]. R^2, R^2_{adj}, the root mean square errors, the mean absolute percentage error, and Akaike's information criterion were used in the evaluation of prediction capacity of MLR models, and these are presented in Table 5.

A model with low RMSE (root mean square error), MAPE (mean absolute percentage error), AIC (Akaike's information

Table 5: ANOVA of d and FA for dependent variable (c-ϕ and CBR).

Parameter	Source	DF	Sum of squares	Mean squares	F	Pr > F
c	Model	2	68661.366	34330.683	79.776	<0.0001
	Error	15	6455.049	430.337		
ϕ	Model	2	756.542	378.271	50.485	<0.0001
	Error	15	112.391	7.493		
CBR	Model	2	138925.972	69462.986	52.921	<0.0001
	Error	51	66941.822	1312.585		

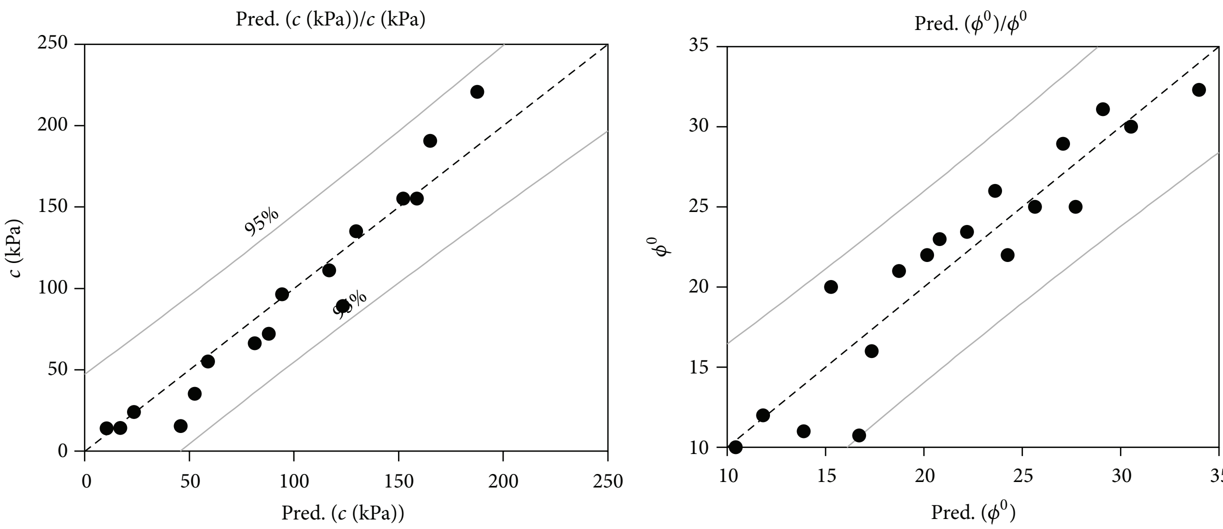

Figure 18: Measured and predicted shear strength (c, ϕ) values derived from (2).

criterion), and high R^2 and adjusted R^2 performance indices was defined, and its prediction capacity was accepted as excellent by several researchers [41–44]. By prediction indices, MLR models have shown good performance for independent variables (Table 6).

Furthermore, measured and predicted shear strength parameters and CBR values obtained from MLR evaluation at the 95% confidence intervals are presented in Figures 18 and 19. Predicted values are in good agreement with the measured values in the laboratory.

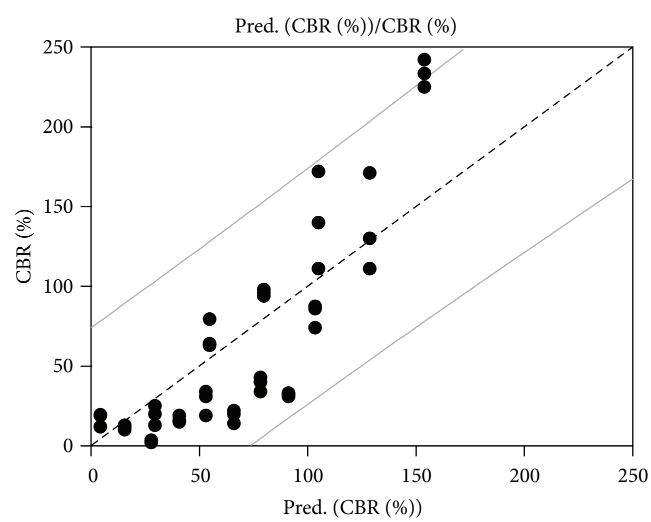

Figure 19: Measured and predicted CBR values derived from (3).

5. Conclusions

By the work reported in this paper, the following conclusions have been drawn:

(1) The liquid and plastic limits of AC were decreased with fly ash addition. Furthermore, the soil class of AC is changed from "CH" to "MH." AC starts showing plastic behaviour when increasing the percentages of FA additives.

(2) The cohesion and internal friction of AC were increased with FA. Furthermore, curing time is very useful on the shear parameters. Soil samples with 28 days' curing time have shown the highest cohesion and friction angle.

(3) SEM views show that FA particles cover the surfaces of clay minerals and constitute an impervious layer. This phenomenon explains why the soil does not swell when FA has been added to it. Furthermore, FA grains build bridges between clay minerals. Therefore, the shear strength (c, ϕ) starts to increase with the FA

Table 6: Goodness-of-fit for MLR.

Dependent variables	Independent variables	R^2	Adj. R^2	RMSE	MAPE	AIC
c	d, FA	0.914	0.903	20.745	47.818	111.880
ϕ	d, FA	0.871	0.853	2.737	11.480	38.969
CBR	d, FA	0.675	0.662	36.23	185.376	390.620

d: curing days; FA: fly ash.

additive increments. Furthermore, there is a robust relationship between shear strength parameters and curing time with fly ash content. Furthermore, the same inference was determined for CBR values.

Competing Interests

The author declares that there are no competing interests.

References

[1] A. Baba, A. Kaya, and Y. K. Birsoy, "The effect of Yatagan thermal power plant (Mugla, Turkey) on the quality of surface and ground waters," *Water, Air, and Soil Pollution*, vol. 149, no. 1–4, pp. 93–111, 2003.

[2] H. Haykiri-Acma, S. Yaman, N. Ozbek, and S. Kucukbayrak, "Mobilization of some trace elements from ashes of Turkish lignites in rain water," *Fuel*, vol. 90, no. 11, pp. 3447–3455, 2011.

[3] G. Akar, M. Polat, G. Galecki, and U. Ipekoglu, "Leaching behavior of selected trace elements in coal fly ash samples from Yenikoy coal-fired power plants," *Fuel Processing Technology*, vol. 104, pp. 50–56, 2012.

[4] A. I. Karayigit, R. A. Gayerb, X. Querol, and T. Onacak, "Contents of major and trace elements in feed coals from Turkish coal-fired power plants," *International Journal of Coal Geology*, vol. 44, no. 2, pp. 169–184, 2000.

[5] S. Esenlik, A. I. Karayigit, Y. Bulut, X. Querol, A. Alastuey, and O. Font, "Element behaviour during combustion in coal-fired Orhaneli power plant, Bursa-Turkey," *Geologica Acta*, vol. 4, no. 4, pp. 439–449, 2006.

[6] S. M. Mackiewicz and E. Glen Ferguson, "Stabilization of soil with self-cementing coal ashes," in *Proceedings of the World of Coal Ash (WOCA '05)*, Lexington, Ky, USA, April 2005.

[7] G. Ferguson, *Use of Self-Cementing Fly Ash as a Soil Stabilizing Agent Fly Ash for Soil Improvement*, GSP no. 36, ASCE Geotechnical Special Publication, 1993.

[8] A. Misra, "Stabilization characteristics of clays using Class C fly ash," *Transportation Research Record*, no. 1611, pp. 46–54, 1998.

[9] J. Prabakar, N. Dendorkar, and R. K. Morchhale, "Influence of fly ash on strength behavior of typical soils," *Construction and Building Materials*, vol. 18, no. 4, pp. 263–267, 2004.

[10] A. J. Puppala and C. Musenda, "Effects of fiber reinforcement on strength and volume change in expansive soils," *Transportation Research Record*, vol. 1736, pp. 134–140, 2000.

[11] A. Senol, T. B. Edil, M. S. Bin-Shafique, H. A. Acosta, and C. H. Benson, "Soft subgrades' stabilization by using various fly ashes," *Resources, Conservation and Recycling*, vol. 46, no. 4, pp. 365–376, 2006.

[12] S. Bin-Shafique, K. Rahman, M. Yaykiran, and I. Azfar, "The long-term performance of two fly ash stabilized fine-grained soil subbases," *Resources, Conservation and Recycling*, vol. 54, no. 10, pp. 666–672, 2010.

[13] P. G. Nicholson and V. Kashyap, "Fly ash stabilization of tropical Hawaiian soils in fly ash for soil improvement," *ASCE Geotechnical Special Publication*, vol. 36, pp. 1134–1147, 1993.

[14] S. Kolias, V. Kasselouri-Rigopoulou, and A. Karahalios, "Stabilisation of clayey soils with high calcium fly ash and cement," *Cement and Concrete Composites*, vol. 27, no. 2, pp. 301–313, 2005.

[15] Y. Du, S. Li, and S. Hayashi, "Swelling-shrinkage properties and soil improvement of compacted expansive soil, Ning-Liang Highway, China," *Engineering Geology*, vol. 53, no. 3-4, pp. 351–358, 1999.

[16] A. A. Langroudi and S. S. Yasrobi, "A micro-mechanical approach to swelling behavior of unsaturated expansive clays under controlled drainage conditions," *Applied Clay Science*, vol. 45, no. 1-2, pp. 8–19, 2009.

[17] D.-F. Lin, K.-L. Lin, M.-J. Hung, and H.-L. Luo, "Sludge ash/hydrated lime on the geotechnical properties of soft soil," *Journal of Hazardous Materials*, vol. 145, no. 1-2, pp. 58–64, 2007.

[18] Z. Nalbantoglu, "Effectiveness of class C fly ash as an expansive soil stabilizer," *Construction and Building Materials*, vol. 18, no. 6, pp. 377–381, 2004.

[19] Z. Nalbantoglu and E. Gucbilmez, "Improvement of calcareous expansive soils in semi-arid environments," *Journal of Arid Environments*, vol. 47, no. 4, pp. 453–463, 2001.

[20] S. M. Rao, B. V. V. Reddy, and M. Muttharam, "The impact of cyclic wetting and drying on the swelling behaviour of stabilized expansive soils," *Engineering Geology*, vol. 60, no. 1–4, pp. 223–233, 2001.

[21] R. N. Yong and V. R. Ouhadi, "Experimental study on instability of bases on natural and lime/cement-stabilized clayey soils," *Applied Clay Science*, vol. 35, no. 3-4, pp. 238–249, 2007.

[22] A. Seco, F. Ramírez, L. Miqueleiz, and B. García, "Stabilization of expansive soils for use in construction," *Applied Clay Science*, vol. 51, no. 3, pp. 348–352, 2011.

[23] L. Chen and D.-F. Lin, "Stabilization treatment of soft subgrade soil by sewage sludge ash and cement," *Journal of Hazardous Materials*, vol. 162, no. 1, pp. 321–327, 2009.

[24] Y. Guney, D. Sari, M. Cetin, and M. Tuncan, "Impact of cyclic wetting-drying on swelling behavior of lime-stabilized soil," *Building and Environment*, vol. 42, no. 2, pp. 681–688, 2007.

[25] P. Sukmak, S. Horpibulsuk, S.-L. Shen, P. Chindaprasirt, and C. Suksiripattanapong, "Factors influencing strength development in clay–fly ash geopolymer," *Construction and Building Materials*, vol. 47, pp. 1125–1136, 2013.

[26] TCLP 1311, *Toxicity Characteristic Leaching Procedure*, US Environmental Protection Agency, Washington, DC, USA, 1992.

[27] American Society for Testing and Materials (ASTM), "Standard test method for shake extraction of solid waste with water," ASTM D3987, American Society for Testing and Materials (ASTM), West Conshohocken, Pa, USA, 1985.

[28] S. Turhan, A. Parmaksiz, A. Köse, A. Yüksel, I. H. Arikan, and B. Yücel, "Radiological characteristics of pulverized fly ashes

produced in Turkish coal-burning thermal power plants," *Fuel*, vol. 89, no. 12, pp. 3892–3900, 2010.

[29] E. Avsar, R. Ulusay, and Z. A. Erguler, "Swelling properties of Ankara (Turkey) clay with carbonate concretions," *Environmental & Engineering Geoscience*, vol. 11, no. 1, pp. 73–95, 2005.

[30] I. Ordemir, C. Soydemir, and A. A. Birand, "Swelling problems of Ankara Clays," in *Proceedings of the 9th International Conference on Soil Mechanics and Foundation Engineering*, pp. 243–247, Tokyo, Japan, July 1977.

[31] TS EN, "Fly ash for concrete-definitions, requirements and quality control," TS EN 450, National Standard, Turkish Standard Institution, Ankara, Turkey, 1998 (Turkish).

[32] TS, "Cement—part1: composition, specification and conformity criteria for common cements," National Standard TS EN 197-1, Turkish Standard Institution, Ankara, Turkey, 2012 (Turkish).

[33] TS 639, *Fly Ashes-Used In Cement Production. National Standard*, Turkish Standard Institution, Ankara, Turkey, 1998 (Turkish).

[34] ASTM C618, *Standard Specification for Coal Fly Ash and Raw or Calcined Natural Pozzolan for Use in Concrete*, American Society for Testing and Materials, West Conshohocken, Pa, USA, 2003.

[35] American Society for Testing and Materials (ASTM), "Standard test methods for laboratory compaction characteristics of soil using modified effort (56,000 ft-lbf/ft^3 (2,700 kN-m/m^3))," ASTM D1557, American Society for Testing and Materials (ASTM), West Conshohocken, Pa, USA, 2009.

[36] ASTM D4318, *Standard Test Methods for Liquid Limit, Plastic Limit, and Plasticity Index of Soils*, American Society for Testing and Materials, West Conshohocken, Pa, USA, 2010.

[37] ASTM D1883, *Standard of Test Method for California Bearing Ratio of Laboratory-Compacted Soils*, American Society for Testing and Materials, West Conshohocken, Pa, USA, 2014.

[38] American Society for Testing and Materials (ASTM), "Standard test method for direct shear test of soils under consolidated drained conditions," ASTM D3080, American Society for Testing and Materials (ASTM), West Conshohocken, Pa, USA, 2004.

[39] IS 2720 (Part XL), *Methods of Test for Soils, Measurement of Swelling Pressure of Soils*, Indian Standard, Delhi, India, 2002.

[40] D. Montgomery and G. Runger, *Applied Statistics and Probability for Engineers*, John Wiley & Sons, New York, NY, USA, 1999.

[41] M. Alvarez Grima and R. Babuška, "Fuzzy model for the prediction of unconfined compressive strength of rock samples," *International Journal of Rock Mechanics and Mining Sciences*, vol. 36, no. 3, pp. 339–349, 1999.

[42] J. Finol, Y. K. Guo, and X. D. Jing, "A rule based fuzzy model for the prediction of petrophysical rock parameters," *Journal of Petroleum Science and Engineering*, vol. 29, no. 2, pp. 97–113, 2001.

[43] C. Gokceoglu, "A fuzzy triangular chart to predict the uniaxial compressive strength of the Ankara agglomerates from their petrographic composition," *Engineering Geology*, vol. 66, no. 1-2, pp. 39–51, 2002.

[44] A. Binal, "Prediction of mechanical properties of non-welded and moderately welded ignimbrite using physical properties, ultrasonic pulse velocity, and point load index tests," *Quarterly Journal of Engineering Geology and Hydrogeology*, vol. 42, no. 1, pp. 107–122, 2009.